



Weak Effect of Membrane Diffusion on the Rate of Receptor Accumulation at Adhesive Contacts.

Olivier Thoumine, Edouard Saint-Michel, Caroline Dequidt, Julien Falk, Rachel Rudge, Thierry Galli, Catherine Faivre-Sarrailh, Daniel Choquet

► To cite this version:

Olivier Thoumine, Edouard Saint-Michel, Caroline Dequidt, Julien Falk, Rachel Rudge, et al.. Weak Effect of Membrane Diffusion on the Rate of Receptor Accumulation at Adhesive Contacts.. *Biophysical Journal*, 2005, 89(5), pp.L40-42. 10.1529/biophysj.105.071688 . hal-00009552

HAL Id: hal-00009552

<https://hal.science/hal-00009552>

Submitted on 5 Oct 2005

HAL is a multi-disciplinary open access archive for the deposit and dissemination of scientific research documents, whether they are published or not. The documents may come from teaching and research institutions in France or abroad, or from public or private research centers.

L'archive ouverte pluridisciplinaire **HAL**, est destinée au dépôt et à la diffusion de documents scientifiques de niveau recherche, publiés ou non, émanant des établissements d'enseignement et de recherche français ou étrangers, des laboratoires publics ou privés.

Weak Effect of Membrane Diffusion on the Rate of Receptor Accumulation at Adhesive Contacts

Olivier Thoumine*, Edouard Saint-Michel*, Caroline Dequidt*, Julien Falk[†], Rachel Rudge[‡], Thierry Galli[‡], Catherine Faivre-Sarrailh[†], and Daniel Choquet*

* CNRS 5091, Université Bordeaux 2, Bordeaux, France; [†] CNRS 6184-NICN, Faculté de Médecine Nord, Marseille, France; [‡] Equipe Avenir, UMR 7592, Institut Jacques Monod, Université Paris VI, Paris, France.

ABSTRACT To assess if membrane diffusion could affect the kinetics of receptor recruitment at adhesive contacts, we transfected neurons with GFP-tagged IgCAMs of varying length (25-180 kD), and measured the lateral mobility of single Quantum Dots bound to those receptors at the cell surface. The diffusion coefficient varied within a physiological range (0.1-0.5 $\mu\text{m}^2/\text{s}$), and was inversely proportional to the size of the receptor. We then triggered adhesive contact formation by placing anti-GFP coated microspheres on growth cones using optical tweezers, and measured surface receptor recruitment around microspheres by time-lapse fluorescence imaging. The accumulation rate was rather insensitive to the type of receptor, suggesting that the long range membrane diffusion of IgCAMs is not a limiting step in the initiation of neuronal contacts.

Received for publication July 29, 2005 and in final form August 17, 2005

Address reprint requests to O. Thoumine, Tel: +33 5 57 5740 91, e-mail: olivier.thoumine@pcs.u-bordeaux2.fr

The formation of adhesive contacts between cells is fundamental in biology. It involves specific adhesion proteins, e.g. IgCAMs which are implicated in neurite elongation and growth cone guidance (1). Contacts are initiated when adhesion molecules find counter-receptors on the surface of neighbouring cells and make selective protein-protein bonds. Such interactions depend on the abundance of receptors expressed by the cells, but also on the ability of receptors to diffuse in the cell membrane (2). The regulation of receptor mobility by cytoplasmic partners, e.g. between L1/neurofascin and ankyrin (3, 4), may then tune the rate at which adhesions form.

To assess if diffusion could affect the kinetics of receptor recruitment at adhesive sites, we used

constructs of varying length (25-180 kD), all tagged extracellularly with GFP. These include L1-GFP, several truncated forms of NrCAM-GFP (5), and GPI-GFP (Fig. 1F). We reasoned that size differences should result in contrasting lateral mobilities. To measure the diffusion coefficient of these receptors, we transfected primary culture neurons and labelled individual receptors with Quantum Dots (QD). Active growth cones were selected for the recordings (Fig. 1A), since these structures are implicated in IgCAM-based locomotion and cell recognition. Around 40% of the receptors were expressed at the plasma membrane (Table 1), allowing QD to bind specifically to transfected cells (Fig. 1B). QD attached to the cell surface and moved in two-dimensions, exploring all

TABLE 1 Surface expression, binding and recruitment of GFP-tagged receptors

Construct	L1	NrCAM	ΔCter	ΔCyto	Δlg	$\Delta\text{lg}\Delta\text{Cyto}$	GPI	GFP
Surface fraction* (%)	35 \pm 7 (14)	46 \pm 10 (12)	34 \pm 8 (16)	40 \pm 4 (10)	46 \pm 6 (16)	44 \pm 12 (14)	48 \pm 8 (15)	4 \pm 3 (16)
# beads per cell*	10.1 \pm 1.0 (40)	4.5 \pm 1.2 (25)	5.7 \pm 0.9 (47)	4.5 \pm 0.8 (34)	5.6 \pm 1.0 (28)	7.1 \pm 1.3 (79)	7.8 \pm 1.8 (67)	0.7 \pm 0.1 (38)
Enrichment factor†	2.6 \pm 0.2 (46)	2.9 \pm 0.2 (37)	3.0 \pm 0.1 (67)	2.5 \pm 0.2 (17)	2.8 \pm 0.1 (47)	2.8 \pm 0.1 (95)	2.9 \pm 0.1 (108)	1.3 \pm 0.1 (18)
Ratio R/L (%)*	22 \pm 6 (9)	24 \pm 7 (11)	18 \pm 5 (7)	26 \pm 6 (9)	26 \pm 4 (8)	25 \pm 8 (8)	25 \pm 5 (10)	2 \pm 1 (9)

All data are expressed as mean \pm sem, where (n) is the number of cells* or beads† examined in each condition. All GFP-tagged receptors are similarly expressed at the cell surface and bind to microspheres, in contrast with GFP alone which remains intracellular.

the growth cone surface (Fig. 1C). Individual QD showed a variety of behaviors, some moving fast, others staying almost immobile. We tracked individual QD and calculated an instantaneous diffusion coefficient for each trajectory.

We thereby obtained a distribution of diffusion coefficients for each construct (Fig. 1D,E) in the range of 0.1-1 $\mu\text{m}^2/\text{s}$ (6). As receptor size diminishes, the distribution shifts to higher mobility values, resulting in a clear inverse relationship between the molecular weight of the receptor and its average diffusion coefficient (Fig. 1G). Since these receptors

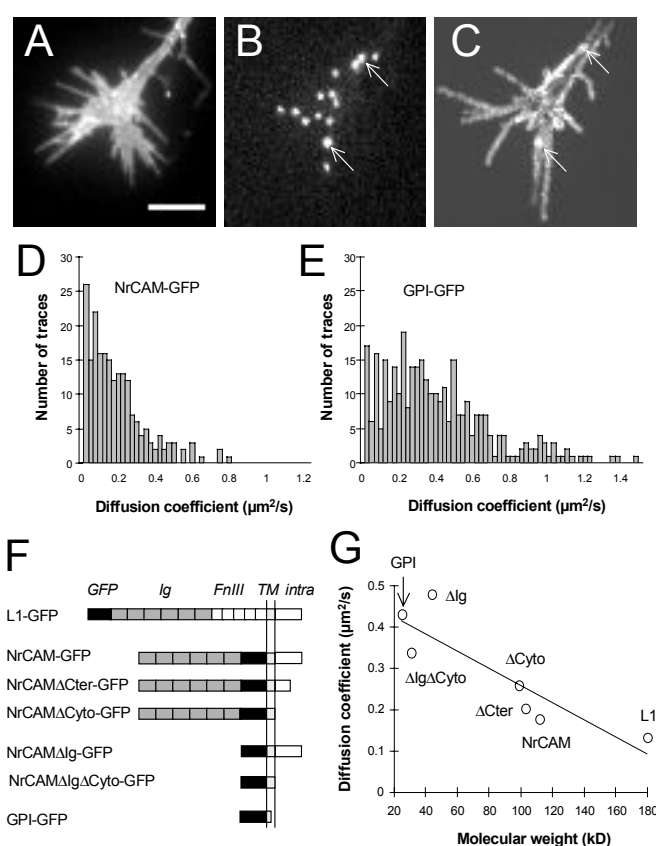


Figure 1. Lateral mobility of GFP tagged receptors. Growth cone expressing NrCAM-GFP (A), labeled with anti-GFP conjugated QD (B). (C) Image of the maximum intensity from the QD channel detected for each pixel along a 1 min sequence, representing the global area explored by QD. Arrows indicate immobile QD. (D) Distributions of the diffusion coefficients for NrCAM-GFP and GPI-GFP. (E) Diagram of the various receptors. In all NrCAM constructs, the fibronectin type III domains have been replaced by GFP: Δ Cter is deleted of the ankyrin binding motif and downstream, Δ Cyto of the entire cytoplasmic tail, Δ Ig of the immunoglobulin domains, and Δ Ig Δ Cyto of both extracellular and intracellular regions. (F) Average diffusion coefficient versus the molecular weight of each construct. The straight line is a linear fit ($r = 0.88$). Bar = 5 μm .

interact similarly with lipid microdomains (5), differences in mobility are unlikely to be associated with variations in the lipid environment. Truncations of intracellular regions caused a slight decrease in lateral mobility (7), which may be attributed to trapping of L1 or NrCAM cytoplasmic tail within the membrane scaffold, or to specific interactions with cytoskeletal partners such as ankyrin or SAP102 (3, 4). Deletions of extracellular regions (FnIII, Ig, or both) strongly reduced receptor diffusion (8). This may be due to steric effects linked to the high glycosylation levels of L1 and NrCAM ectodomains. Alternatively, IgCAMs with intact FnIII and/or Ig domains are able to interact in cis with themselves or other receptors (1), thus forming complexes with lower diffusion properties.

We then mimicked adhesive contacts using anti-GFP coated latex microspheres, which selectively bound to transfected cells (Fig. 2A,B; Table 1) and recruited GFP-tagged membrane receptors (Fig. 2C,D). We placed microspheres on growth cones using optical tweezers, and followed the accumulation of receptors around them (Fig. 2E). We quantified the ratio between the fluorescence level on the microsphere and that on adjacent regions. This enrichment factor increased in a few minutes, slightly faster for smaller receptors (Fig. 2F), and reached a plateau around 3 with minor differences between the constructs (Table 1). That equilibrium value corresponded to the saturation of antibody binding sites on microspheres by GFP-tagged receptors.

We modeled the receptor recruitment data using first order kinetics: $dC/dt = k_{on}(R-C)(L-C) - k_{off}C$, where R is the receptor density at the cell surface ($\approx 1000/\mu\text{m}^2$), L the density of GFP binding sites on microspheres ($\approx 4000/\mu\text{m}^2$), C the surface density of bonds between antibodies and receptors, and k_{on} and k_{off} the forward and reverse rate constants, respectively. Fluorescence measurements outside bead contacts indicated that there was no receptor depletion, so we took $(R-C)=R$. Furthermore, antibody-antigen bonds being very stable, we set $k_{off} = 0$. This left equation [1]: $C(t) = L[1-\exp(-k_{on}Rt)]$, which was used to fit the data and gave the two parameters R/L (Table 1) and $k_{on}R$.

The association rate $k_{on}R$ increased weakly with the receptor diffusion coefficient (Fig. 2C), showing that receptor accumulation at microsphere contacts is not diffusion-limited. This agreed with a theoretical model taking into account the long-range diffusion of

receptors towards a narrow zone where they can be irreversibly trapped by immobilized ligands (9). Beads coated with lower affinity ligands such as mAb against GFP (not shown), TAG-1 (5), or N-cadherin (10) all induced slower accumulation of counter-receptors, suggesting that the adhesive reaction is the limiting step there. Thus, there appears to be a large enough reservoir of highly diffusive IgCAMs that can be mobilized quickly at adhesive sites, waiting for ligand binding. It is still possible that subtle differences in the diffusion of less mobile receptor complexes, controlled locally by the cytoskeleton or the lipid environment, can modulate the initiation and durability of neuronal interactions.

EXPERIMENTAL METHODS

Methods are provided as online supplemental material on the BJ website <http://www.biophysj.org>.

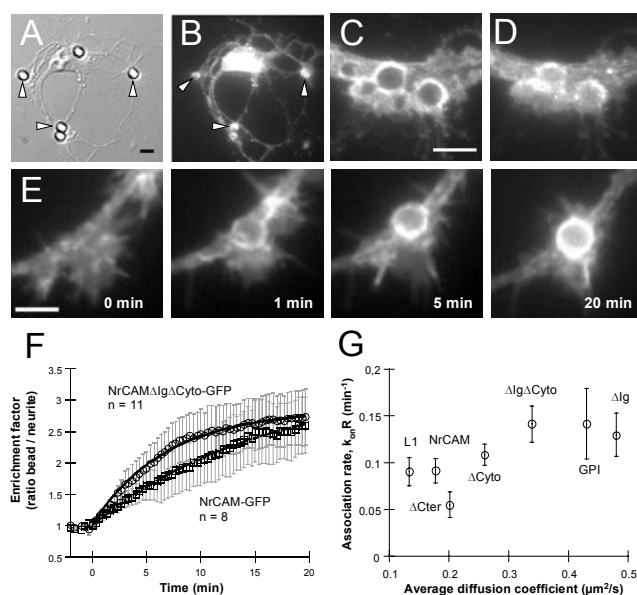


Figure 2. Kinetics of GFP-tagged receptor trapping. (A-D) Neurons transfected for NrCAM-GFP were incubated for 1 hr with 4 μm anti-GFP coated microspheres. (A) DIC image, (B) GFP channel. Arrow heads indicate bound beads which have recruited NrCAM-GFP. (C, D) Higher magnification views showing the recruitment of NrCAM-GFP (C), and a corresponding surface anti-HA immunostaining (D). (E) Time sequence of NrCAM-GFP accumulation around a microsphere placed on a growth cone for 10 sec at time zero. (F) Individual data showing the enrichment factor versus time for NrCAM-GFP and NrCAM $\Delta\text{Ig}\Delta\text{Cyto}$ -GFP (mean \pm sem). The plain curves represent fits with equation [1]. (G) Rate constant k_{onR} versus the diffusion coefficient for all receptors ($n = 8$ -12 experiments for each construct). Bars = 5 μm .

ACKNOWLEDGMENTS

We thank S. Mayor for the gift of GPI-GFP, V. Racine and J.B. Sibarita at Institut Curie for the peak detection algorithm, L. Cognet for tracking routines, and C. Breillat and D. Bouchet for dissections and molecular biology. We acknowledge financial support from CNRS, French Ministry of Research, and INSERM.

REFERENCES

1. Brummendorf, T. and Lemmon, V. 2001. Immunoglobulin superfamily receptors: cis-interactions, intracellular adapters and alternative splicing regulate adhesion. *Curr Opin Cell Biol.* 13, 611-8.
2. Lauffenburger, D. A. and Linderman, J. J. 1993. Receptors: models for binding, trafficking, and signaling, Oxford University Press, New York.
3. Garver, T. D., Ren, Q., Tuvia, S. and Bennett, V. 1997. Tyrosine phosphorylation at a site highly conserved in the L1 family of cell adhesion molecules abolishes ankyrin binding and increases lateral mobility of neurofascin. *J Cell Biol.* 137, 703-14.
4. Gil, O. D., Sakurai, T., Bradley, A. E., Fink, M. Y., Cassella, M. R., Kuo, J. A. and Felsenfeld, D. P. 2003. Ankyrin binding mediates L1CAM interactions with static components of the cytoskeleton and inhibits retrograde movement of L1CAM on the cell surface. *J Cell Biol.* 162, 719-30.
5. Falk, J., Thoumine, O., Dequidt, C., Choquet, D. and Faivre-Sarrailh, C. 2004. NrCAM coupling to the cytoskeleton depends on multiple protein domains and partitioning into lipid rafts. *Mol Biol Cell.* 15, 4695-709.
6. Simson, R., Yang, B., Moore, S. E., Doherty, P., Walsh, F. S. and Jacobson, K. A. 1998. Structural mosaicism on the submicron scale in the plasma membrane. *Biophys J.* 74, 297-308.
7. Edidin, M., Zuniga, M. C. and Sheetz, M. P. 1994. Truncation mutants define and locate cytoplasmic barriers to lateral mobility of membrane glycoproteins. *Proc Natl Acad Sci U S A.* 91, 3378-82.
8. Zhang, F., Crise, B., Su, B., Hou, Y., Rose, J. K., Bothwell, A. and Jacobson, K. 1992. The lateral mobility of some membrane proteins is determined by their ectodomains. *Biophys J.* 62, 92-4.
9. Crank, J. 1975. The mathematics of diffusion, Oxford University Press, New York.
10. Thoumine, O., Lambert, M., Mège, R. and Choquet, D. 2005. Regulation of N-cadherin dynamics at neuronal contacts by ligand binding and cytoskeletal coupling. *Mol Biol Cell.*, in press.